Distortion effects in a relativistic one-nucleon model for the (p,π^+) reaction

E. D. Cooper* and H. S. Sherif
Nuclear Research Centre, University of Alberta, Edmonton, Alberta, Canada T6G 2N5
(Received 21 January 1982)

A relativistic distorted-wave Born approximation model is developed for (p,π^+) reactions within the framework of the one-nucleon mechanism. The nucleon motion is described by solutions to the Dirac equation with appropriate nuclear potentials. Distortion effects in both the proton and pion channels are taken into account and are found to be important. Both pseudovector and pseudoscalar forms of the πNN vertex are considered. The former is found to lead invariably to better agreement with the data. Calculations have been carried out for proton energies ≤ 200 MeV. Good agreement is obtained with the cross section data for reactions on ^{40}Ca and ^{16}O leading to the ground state of the residual nucleus. For reactions on ^{12}C, the cross section shapes, but not their magnitudes, are reproduced. The calculated analyzing powers are found to be in good agreement with the forward angle data.

[NUCLEAR REACTIONS $(\vec{p},\pi^+)$ reaction, relativistic one-nucleon model, DWBA, Dirac phenomenology, pseudovector and pseudoscalar πNN vertex, calculated $\sigma(\theta)$ and $A_y(\theta)$, comparison with experiment.]

I. INTRODUCTION

Owing to the high momentum transfer involved in (p,π^+) reactions, it has been hoped that these reactions would yield valuable information on the high momentum components of nuclear wave functions. These hopes have not yet been realized, due to a lack of understanding of the underlying reaction mechanism. Currently there are two proposed models for the reaction,[1,2] known as the one nucleon model (ONM) and the two nucleon model (TNM). Among these, the TNM is the more sophisticated one, at least in that it is closer to a microscopic description of the process. It is based on the assumption that the incident proton interacts with a target nucleon, producing two nucleons and a pion. These two nucleons end up in bound nuclear orbits while the pion is set free. The TNM calculations have several difficulties associated with them.[3-5] There is, in general, a nine-dimensional integral to be done. The $NN \rightarrow NN\pi$ amplitudes are required off shell, for which a model must be used. Such a model would undoubtedly introduce more uncertainty into the calculations. Double counting of distortion effects can be a problem and, finally, since three nucleon wave functions are involved, information on the high momentum components of each one is not directly accessible. On the more optimistic side, the assumption of a Δ dominance[6] for proton energies above 200 MeV simplifies the calculations. A simple phenomenological model by Ruderman,[7] later reexamined and expanded to include distortion effects by Fearing,[8] has been successful in interpreting the data on light target nuclei, such as ^{2}H and ^{3}He, for incident proton energies in the range from 350 to 600 MeV. These calculations can generally reproduce the shape of the angular distributions and for energies near 470 MeV give the correct normalization to within a factor of 2. The Fearing-Ruderman model has not been applied to heavier nuclei, mainly because one of the basic ingredients of the model is the dominant presence of a deuteron cluster in the final nuclear state, which is improbable for these nuclei. In addition, this model has not yet been tested in terms of its predictions for the analyzing power.

In the ONM (also referred to as pionic stripping model) it is assumed that the pion is emitted by the incident proton only. The ONM can easily be treated in a distorted wave Born approximation (DWBA) framework, in which distortion effects in both the incident and final channels are accounted for. Despite the many efforts devoted to these (nonrelativistic) DWBA calculations in recent years, the results have generally been rather disappointing. In particular, these calculations appear to suffer from two major difficulties.[1] One of these is the extreme sensitivity to the not-so-well known pion-nucleus optical potential. Another major problem is the ambiguity concerning the nonrelativistic transition

operator. In a recent study of the nonrelativistic ONM, Tsangarides *et al.*[9,10] examined, in detail, the effects of this vertex ambiguity. The most commonly used form of the vertex is given by

$$H_{\pi NN}=(f/m_\pi)[\vec{\sigma}\cdot\vec{\nabla}_\pi(\vec{\tau}\cdot\vec{\phi}_\pi) -\lambda(m_\pi/M)(\vec{\tau}\cdot\vec{\phi}_\pi)\vec{\sigma}\cdot\vec{\nabla}_p] . \quad (1)$$

Here λ is an arbitrary constant arising from a unitary transformation ambiguity in the Foldy-Wouthuysen reduction of the pseudoscalar vertex.[11,12] Tsangarides finds that no value of λ can simultaneously explain the cross section and analyzing power data. Specifically, the "Galilean invariant" form ($\lambda=1$) gives a reasonable account of the cross sections but gives analyzing powers of the opposite sign to the data, whereas the "static" ($\lambda=0$) form gives analyzing powers of the correct sign, but often fails to reproduce the shape of the differential cross sections. Various other forms of this vertex have been given. Friar[12] gives a form of the vertex which does not seem to lead to ambiguities in the T-matrix elements, although as pointed out by Lee and Pittel,[13] the ambiguity (i.e., sensitivity to λ) remains if the outgoing pion is allowed to rescatter.

Pionic stripping calculations have also been performed using Dirac spinors for the incident proton and bound neutron.[14,15] The advantage of such calculations is that the vertex can be taken directly from a relativistic theory, without the need for a nonrelativistic reduction, hence avoiding any possible ambiguity that might arise in the process. These calculations neglected distortion effects in the incident and exit channels. Comparisons with the nonrelativistic PWBA calculations indicated that the predicted cross sections can differ by more than an order of magnitude. Miller and Weber[16] have made a preliminary attempt to include distortion effects in this type of calculation. They found that pion distortion effects were rather important while proton distortion effects were not. As we show below, this latter conclusion is not borne out by our present study, and appears to have been an artifact of the manner in which these distortion effects have been taken into account.

We present here a detailed account of a relativistic DWBA treatment[17] of the reaction in which distortion effects are handled properly. The stripping calculations are done in the zero range DWBA framework. The pion distorted waves are calculated in a straightforward manner using a standard optical potential.[18] The Dirac equation is used to describe the nucleon motion and hence the lower components of the wave function are treated explicitly. In the incident channel the proton waves are distorted by complex vector and scalar potentials which properly describe the proton elastic scattering on the target nucleus. To our knowledge, this is the first time such distorted waves have been used in a nuclear reaction calculation. The neutron bound state wave function is generated in a similar fashion using real potentials.[19–22] In Sec. II we give some details of the calculations and elaborate on the methods of generating the wave functions involved. We also show, in the present context, that the pseudoscalar vertex leads to results different from those with the pseudovector vertex, and discuss the connection to the equivalence theorem.[23,24] In Sec. III we present some detailed results and comparisons with experimental data, and discuss the prominent features of our model. We present some concluding remarks in Sec. IV.

II. FORMALISM AND CALCULATIONAL DETAILS

We consider the case of a (p,π^+) reaction on an even-even target nucleus with equal numbers of protons and neutrons. The residual nuclear state is a single particle state built on the target as an inert core (for simplicity, we assume a spectroscopic factor of unity). In the zero-range distorted wave Born approximation, the t-matrix elements are given by

$$T=i\sqrt{2}\int d^4x\,\bar{\Psi}_{J_bM_b}(x)\Gamma(x)\Psi^{(+)}_{\mu_i}(x)\phi^{*(-)}_\pi(x) , \quad (2)$$

where $\Psi^{(+)}_{\mu_i}(x)$ is the proton distorted wave with the subscript μ_i referring to the initial spin projection, $\phi_\pi(x)$ is the pion distorted wave, and $\Psi_{J_bM_b}(x)$ is the neutron bound state wave function with angular momentum J_b and projection M_b. Both $\Psi_{\mu_i}(x)$ and $\Psi_{J_bM_b}(x)$ are obtained by solving Dirac equations of the form

$$i\gamma^\mu\partial_\mu\Psi(x)=[M+U_s(r)+\gamma^0U_v(r)]\Psi(x) , \quad (3)$$

where $U_s(r)$ and $U_v(r)$ are nuclear potentials which transform as a Lorentz scalar and as the timelike component of a Lorentz four-vector, respectively. For the bound neutron these potentials are real, while for the incident proton they are complex and also include the Coulomb potential as part of the vector interaction. The vertex $\Gamma(x)$ is taken to be of either pseudoscalar (PS) or pseudovector (PV) type,

$$\Gamma(x)=\begin{cases} g\gamma_5, & \text{PS} \\ -i(g/2M)\gamma_5\gamma^\mu\partial^{(\pi)}_\mu, & \text{PV} , \end{cases} \quad (4)$$

where g is the coupling constant; $g^2/4\pi = 14.6$.

In order to clarify the relationship between the above two types of vertex, we proceed as follows. Consider the case of PV coupling. Starting from the Dirac Eq. (3) for the proton spinors and the Hermitian conjugate equation for the neutron spinors, we integrate Eq. (2) by parts. This enables us to get rid of the derivative terms and replace them by expressions involving the nuclear potentials. Upon ignoring a small recoil term (which is included in the final calculations), the resulting t-matrix elements can be written as:

$$T^{\mathrm{PV}} = (ig/\sqrt{2}M)\int d^4x\, \bar{\Psi}_{J_bM_b}(x)\gamma_5[2M + U_s^p(r) + U_s^n(r) + \gamma^0(U_v^p(r) - U_v^n(r))]\Psi_{\mu_i}^{(+)}(x)\phi_\pi^{*(-)}(x) \ . \tag{5}$$

The superscripts p and n on the potentials refer to the incident proton and the bound neutron, respectively.

The corresponding result for PS coupling can be obtained from the one above by replacing the square bracket by $2M$. Thus we may write

$$T^{\mathrm{PS}} = T^{\mathrm{PV}} - (ig/\sqrt{2}M)\int d^4x\, \bar{\Psi}_{J_bM_b}(x)\gamma_5\left(U_s^p(r) + U_s^n(r) + \gamma^0(U_v^p(r) - U_v^n(r))\right)\Psi_{\mu_i}^{(+)}(x)\phi_\pi^{*(-)}(x) \ . \tag{6}$$

From the above expression, we see that the PV-PS equivalence is broken by virtue of the presence of the nuclear interactions. Our result is in general agreement with the conclusions made by Friar,[23] who has discussed this equivalence in the presence of scalar, vector, as well as tensor interactions (the latter type is not considered in our present treatment). A closer look at Eq. (6) reveals that the PS and PV couplings give the same result in the limit of both scalar potentials vanishing and the two vector potentials being equal. For a real nucleus, however, the scalar potentials are several hundred MeV in depth. Furthermore, in the DWBA framework the continuum state potentials are complex and hence differ radically from those of the bound state. As a consequence we do not expect the PV-PS equivalence to hold in the present model. We note, however, that Noble[24] has shown that when PS coupling is treated in the framework of the $\sigma + \omega$ model [which complies with partial conservation of axial-vector currents (PCAC)] then the equivalence is largely restored.

The bound state wave function is written in terms of its upper and lower components as follows[16]:

$$\Psi_{J_bM_b}(\vec{r}) = \begin{bmatrix} F_b(r)\ \mathscr{Y}^{M_b}_{L_b\,1/2\,J_b}(\Omega) \\ -iG_b(r)\ \mathscr{Y}^{M_b}_{L_b'\,1/2\,J_b}(\Omega) \end{bmatrix} , \tag{7}$$

where the $\mathscr{Y}$'s are generalized spin-$\frac{1}{2}$ spherical harmonics, L_b is the orbital angular momentum of the state, and $L_b' = 2J_b - L_b$.

We similarly express the proton distorted waves in terms of upper and lower components, and further make a partial wave expansion of both these as well as the pion distorted waves. Then after carrying out the angular momentum algebra, the final expression for the t matrix for PV coupling can be written as (without the energy conserving δ function)

$$\begin{aligned} T^{\mathrm{PV}} = (g/2\pi)\sqrt{2J_b+1}(-)^{1/2+M_b}\sum_{lLJM} i^{L-l}[(2J+1)/(2l+1)]^{1/2} Y_L^{*M-\mu_i}(\hat{k}_p)Y_l^m(\hat{k}_\pi) \\ \times (L\tfrac{1}{2};M-\mu_i\mu_i \mid JM)(J_bJ;-M_bM \mid lm) \\ \times (J_bJ;\tfrac{1}{2}-\tfrac{1}{2} \mid lo)(I_1P(L_b,l,L') + I_2P(L_b',l,L)) \ , \end{aligned} \tag{8}$$

where L and l refer to the proton and pion partial waves, respectively, and $L' = 2J - L$. The P's are parity coefficients

$$P(L_b,l,L') = \tfrac{1}{2}(1 + (-)^{L_b+l+L'}) \ . \tag{9}$$

I_1 and I_2 are radial integrals given by

$$\begin{aligned} I_1 = (2M)^{-1}\int_0^\infty F_b(r)(2M + U_s^p + U_s^n + U_v^n - U_v^p) \\ \times G_{LJ}(r)f_l(r)r^2dr \end{aligned} \tag{10}$$

and

$$\begin{aligned} I_2 = (2M)^{-1}\int_0^\infty G_b(r)(2M + U_s^p + U_s^n - U_v^n + U_v^p) \\ \times F_{LJ}(r)f_l(r)r^2dr \ . \end{aligned} \tag{11}$$

Here F_{LJ} (G_{LJ}) are the upper (lower) radial components of the proton partial waves and f_l is the radial part of the pion partial wave. As before, the corresponding results for PS coupling are obtained from the above expressions by dropping the nuclear

potential terms in Eqs. (10) and (11).

One feature of interest in the above equations is the way in which the lower components of the nuclear wave functions enter the expressions for the radial integrals. In each of these integrands there is a product of a lower and an upper component; thus the former participates on equal footing in the determination of the reaction amplitude. This makes us a little suspicious of any nonrelativistic calculation in which the presence of the lower components is not properly accounted for.

In what follows we outline how the wave functions appearing in the above expressions are calculated and discuss some of the relevant aspects of these calculations.

A. The bound-state wave function

As pointed out above, this wave function is taken as a Dirac spinor which is a solution to a Dirac equation with a potential consisting of an attractive scalar part and a repulsive vector part. Since Dirac Hartree Fock calculations[19,21] have indicated that these potentials tend to follow the nuclear shape, we represent them here by Woods-Saxon functions.[20] It follows that we have, in principle, six parameters that may be varied in order to determine the appropriate bound state wave functions. In the present work we follow an approach in which the geometry parameters are fixed and only the depth parameters V_s and V_v are varied. For calcium, the choice of the geometry parameters is dictated by the corresponding values obtained from consideration of elastic scattering in the incident channel (see below). For simplicity we used an average geometry for both the vector and scalar potentials since in practice it made little difference from the case of two separate geometries. For oxygen and carbon, since we did not expect these parameters to be very well determined by the elastic scattering data, we have adopted a geometry of $r=1.0$ fm and $a=0.4$ fm. (r is the radial parameter and a the diffuseness.) The depth parameters V_v and V_s of the vector and scalar potentials were further constrained to have a ratio $V_v/V_s=-0.81$ which is suggested by the work of Walecka[25] and appears to be supported by extrapolations from results of proton elastic scattering.[26] The specific magnitudes of V_v and V_s are finally determined by requiring that they reproduce the correct binding energy of the single particle state as well as the correct number of nodes of the radial wave function.

The role of the lower component of the bound state wave function in (p,π^+) reactions can be made clear from an inspection of Fig. 1. The figure shows the momentum space wave functions for the $1f_{7/2}$ neutron in ^{41}Ca. The geometry parameters used in this calculation are a radius parameter $r=1.0$ fm and a diffuseness $a=0.65$ fm. The depth parameters determined from the procedure mentioned in the preceding paragraph are $V_v=453$ MeV and $V_s=-560$ MeV. The region of momentum transfer pertinent to pion production on ^{40}Ca with 160 MeV protons is indicated by the horizontal arrow. We note that in this region, unlike the situation at small momentum transfer, the magnitude of the lower component of the wave function can overtake that of the upper component. We no longer can regard the lower component as the "small" component. This fact delineates the importance of adopting a relativistic approach to (p,π^+) reactions.

B. The proton distorted wave

The proton distorted waves are solutions of the Dirac Eq. (2). In this instance the proton-nucleus interactions are described by complex vector and scalar potentials whose parameters are determined from a fit to the elastic scattering data. This Dirac equation based approach has met with reasonable success in describing proton-nucleus elastic scatter-

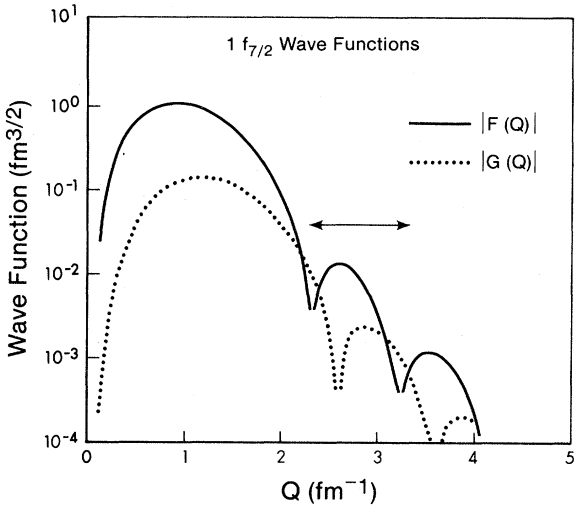

FIG. 1. The momentum-space wave functions for the $1f_{7/2}$ neutron orbit in ^{41}Ca. $F(Q)$ is the upper component and $G(Q)$ the lower component of the wave function. The arrow indicates the region of momentum transfer pertaining to the ^{40}Ca$(p,\pi^+)^{41}$Ca reaction for $T_p=160$ MeV.

ing at intermediate energies.[26–28] A computer search code RUNT has been developed in the course of the present work. RUNT calculates the phase shifts and elastic observables in the usual manner. The potential parameters are automatically varied so as to fit the proton elastic scattering data. The potentials determined by RUNT are used to generate proton distorted waves for use in the DWBA calculations. We have used this code to analyze various data for proton energies in the range 100–500 MeV on various nuclei. Among them are data for energies and nuclei for which (p,π^+) data exist. The search program has produced two distinct classes of potentials that fit the elastic scattering data. These two classes, which we refer to as classes *A* and *B*, have similar real parts; however, their imaginary parts are very different. Class *A* type solutions, with general characteristics similar to those of Arnold, Clark, and co-workers,[26–28] have very large imaginary potential well depths which have opposite signs. In particular, the imaginary well of the vector potential is very absorptive whereas the imaginary part of the scalar potential is large and creates flux. Class *B* solutions, on the other hand, are characterized by small absorptive imaginary depths. The differences between these two types of potentials will be discussed in more detail in a separate publication.[29] For the moment, it suffices to say that we have performed (p,π^+) reaction calculations using both classes and will present samples of each of them in Sec. III. Figure 2 shows the quality of fits obtained for the elastic scattering data using the class *B* potentials, in this instance for the case of 181.3 MeV protons scattered by ^{40}Ca. Generally these class *B* fits are only slightly superior to the corresponding class *A* fits.[27]

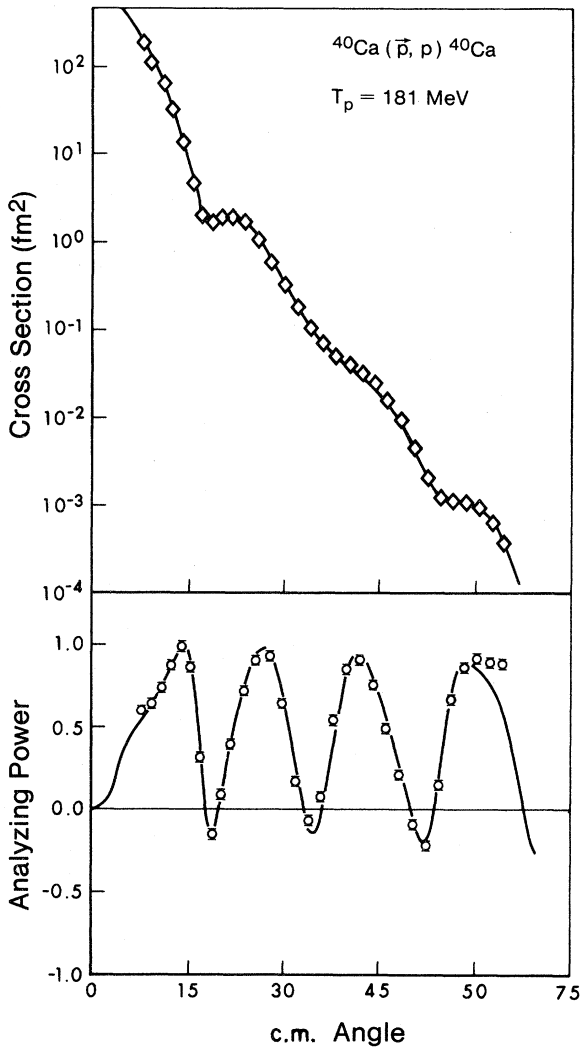

FIG. 2. Cross sections and analyzing powers for the elastic scattering of 181 MeV protons on ^{40}Ca. The data are from Ref. 27. The solid curves are relativistic optical model fits using class *B* type parameters as described in the text.

C. The pion distorted wave

The pion wave function is a solution to a Klein-Gordon equation which incorporates an appropriate pion-nucleus optical potential. In the present work we use the potential of Stricker *et al.*[18] which is based on analyses of pionic atom data and reproduces the pion elastic scattering data up to 50 MeV. This potential has also been used recently in studies of pion inelastic scattering[30] and in pion radiative capture reactions.[31] Nonrelativistic DWBA calculations have shown great sensitivity to the type of pion distorting potential used. We have not yet addressed the question of whether this sensitivity persists in the relativistic calculations; however, we note in this regard that small changes in the parameters of the potential used here do not cause any significant changes in our (p,π^+) calculations.

III. RESULTS AND DISCUSSION

In nonrelativistic DWBA calculations, it has been found that the calculated (p,π^+) observables are sensitive to distortion effects in both the pion and proton channels. We begin this section with a discussion of these effects in the case of the present relativistic treatment. We show in Fig. 3 various types of calculation, using PV coupling, for the

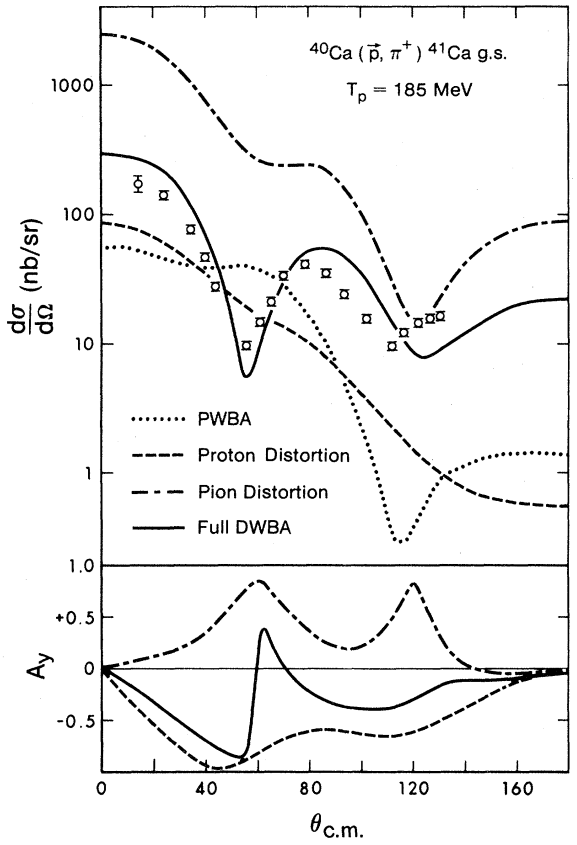

FIG. 3. Distortion effects on the calculated cross sections and analyzing powers for the reaction $^{40}Ca(\vec{p},\pi^+)^{41}Ca(g.s.)$ at $T_p = 185$ MeV. The curves are calculated using PV coupling for the following cases: (i) no distortion in either pion or proton channels (dotted curve), (ii) distortion in the proton channel only (dashed curve), (iii) distortion in the pion channel only (dashed-dotted curve), and (iv) distortion in both proton and pion channels (solid curve). The cross section data shown are taken from Ref. 32.

cross section and analyzing power in the reaction $^{40}Ca(p,\pi^+)^{41}Ca(g.s.)$ at 185 MeV. For comparison purposes we also show the cross section data of Dahlgren *et al.*[32]

From the upper part of Fig. 3 we note that pion distortion alone (dashed-dotted curve) increases the cross section compared to the plane wave result (dotted curve) by nearly an order of magnitude. On the other hand, proton distortion (dashed curve) merely leads to a smearing out of the angular distribution. None of the above calculations shows much resemblance to the data. The solid curve (labeled full DWBA) shows the result of including both pion and proton distortions. It can be seen that this curve is quite different from the other three. It appears from this comparison that in the presence of pion distortion, proton distortion acquires added importance and can cause significant changes in the predicted cross sections. Moreover, without the pion rescattering, the differential cross section loses all its structure. Finally, we note that when both distortion effects are included the general characteristics of the observed cross sections are fairly well reproduced. The process of turning on the potentials one at a time has also been carried out at 160 and 148 MeV. The outcome at these lower energies is as dramatic as at 185 MeV. In particular, the absence of pion distortion results in the calculated curves losing all their structure, and becoming monotone decreasing as a function of angle.

The lower part of Fig. 3 illustrates the effects of distortion on the calculated analyzing power. The plane-wave result is identically zero everywhere and thus is not shown. When only pion distortion is included (dashed-dotted curve), the resulting analyzing power is dominantly positive whereas that with proton distortion only (dashed curve) is negative over the entire angular range. When both distortion effects are included (solid curve) the resulting analyzing power is still dominantly negative. This indicates that proton distortion plays a key role in determining the analyzing power with pion distortion modifying its shape to some extent.

The preceding general remarks concerning distortion effects also hold in much the same fashion for the case of PS coupling. There is one important difference, however, between PV and PS results. We find that, providing one carries out a full DWBA calculation, the PV coupling results are in much better accord with the data than those with PS coupling. This point is illustrated further by the comparisons of Fig. 4, where we show predictions for the reaction in question, at three different proton energies. The experimental data are those of Dahlgren *et al.*[32] and Pile *et al.*[33] In all cases we find that, even though the angular distributions with PV and PS coupling have much in common, the PS curves are generally out of phase with the observed data. For PV coupling the agreement with the data is quite good at 160 and 185 MeV; however, at 148 MeV the minimum is in the wrong place. This is possibly due to not having the correct proton distortion; since no proton elastic scattering data exist at 148 MeV, we have had to use the parameters obtained from fitting the 160 MeV elastic data.[34] It turns out that if we use a class *A* potential based on a fit to the 160 MeV data for the

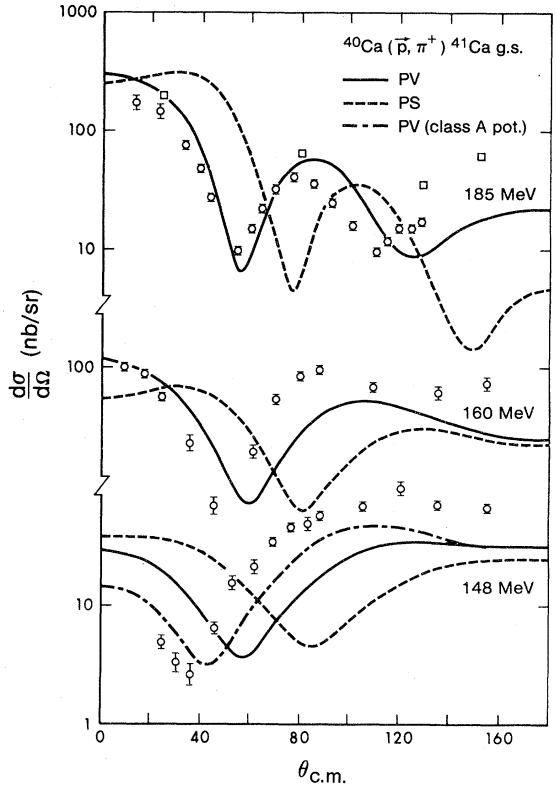

FIG. 4. Cross sections for the reaction $^{40}Ca(\vec{p},\pi^+)^{41}Ca(g.s.)$ at $T_p=185$, 160, and 148 MeV. The solid curves are calculated using PV coupling, the dashed curves using PS coupling; in both cases class B proton potentials are used. The dashed-dotted curve for $T_p=148$ MeV is obtained using PV coupling and class A proton potentials. The data points at 185 MeV are open circles (Ref. 32) and open squares (Ref. 33 at $T_p=182.5$ MeV). The data at 160 and 148 MeV are from Ref. 33.

proton distorted waves at 148 MeV, then the minimum in the (p,π^+) cross section moves towards the correct position as is shown by the dashed-dotted curve in Fig. 4. This gives us a measure of the uncertainties in the (p,π^+) calculations which may arise from ambiguities in the proton distortion potentials where proton elastic scattering data do not exist.

We have carried out similar calculations for the reaction $^{16}O(p,\pi^+)^{17}O(g.s.)$. The cross sections for this reaction have been measured by Dahlgren *et al.*[32] using 185 MeV protons and by Sjoreen *et al.*[35] for proton energies in the range 154–183 MeV. The analyzing power has also been measured at $T_p=157$ MeV.[36] Because of a general lack of proton elastic scattering data on oxygen in this energy range, the optical potentials used to generate the proton distorted waves are not as well determined as for the ^{40}Ca case. Calculations in the energy range 154–165 MeV were carried out using potential parameters determined from a fit to the 155 MeV elastic polarization data of Alphonce *et al.*[37] For $T_p=185$ MeV, the parameters were determined from fits to preliminary data from TRIUMF for proton scattering on ^{16}O at 200 MeV.[38] In both cases the potentials are of the class A variety mentioned above. The geometry parameters for the $1d_{5/2}$ bound state wave function are $r=1.0$ fm and $a=0.4$ fm. Other geometry parameters were tried but the resulting changes in the angular distributions were either not significant or lead to inferior results. This geometry also has the interesting feature that both the radial parameter and the potential depths are the same as for the $1f_{7/2}$ orbital in ^{41}Ca. As with all calculations reported here we assume a spectroscopic factor of 1.0. In Fig. 5 we show the results of our calculations for four proton energies from 154 to 185 MeV. The solid curves are calculated using the pseudovector coupling vertex. It is seen that there is general agreement with the data at forward angles. The minimum comes out at the right place for the 185 MeV distribution and the calculation predicts the correct sense of the shift of the minimum but overestimates this shift. The calculations do not do as well at back angles in that they underestimate the cross section particularly at the lower proton energies. For comparison we also show the results for pseudoscalar coupling at the highest and lowest proton energies. It is evident, as was the case in ^{40}Ca, that these results are inferior to the PV coupling ones. They overestimate the cross section magnitudes and at 185 MeV show a minimum that is shifted by some 40° with respect to the one observed. Even if a realistic spectroscopic factor is used, which will reduce the calculated cross sections by approximately 20%, the PV curves will still be superior.

In Fig. 6 we show the analyzing power for the same reaction at 157 MeV. The data points are those of Sjoreen *et al.*[36] The solid curve, depicting the PV coupling calculation, shows some qualitative accord with the data; in particular, the calculated analyzing power is large and negative in the forward hemisphere. This feature is a dominant characteristic of analyzing power data (see discussion of ^{12}C results below) and is generally predicted by our calculations. The dashed curve in Fig. 6 shows the analyzing power calculated using the PS coupling. In this case the calculated A_y is much too

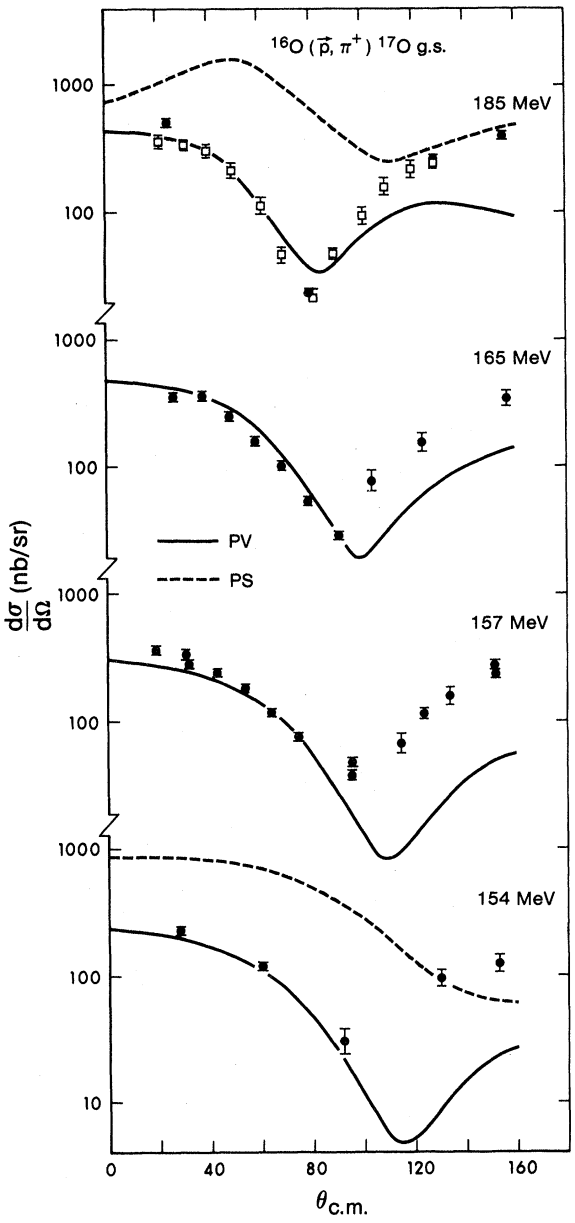

FIG. 5. Cross sections for the reaction $^{16}O(\vec{p},\pi^+)^{17}O$(g.s.) at $T_p=185$, 165, 157, and 154 MeV. The solid curves are calculated using PV coupling, the dashed curves using PS coupling. The solid circles are data taken from Ref. 35 and the open squares are from Ref. 32.

small at forward angles, but appears to be in better agreement with the data at large angles.

Whatever success we have in dealing with ground state transitions for the ^{40}Ca and ^{16}O targets, unfortunately does not extrapolate to excited states. Calculations for the 0.87 MeV state in ^{17}O in the same proton energy range result in angular distributions

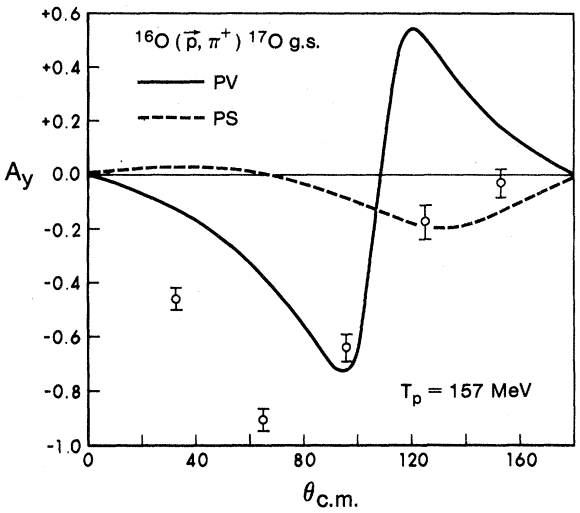

FIG. 6. The analyzing powers for the reaction $^{16}O(\vec{p},\pi^+)^{17}O$(g.s.) at $T_p=157$ MeV. The solid curve is calculated using PV coupling, the dashed curve using PS coupling. The data are taken from Ref. 36.

that agree in shape with those observed, but which are an order of magnitude smaller. We have encountered the same feature in dealing with reactions on ^{12}C. We present here results of calculations carried out for the reaction $^{12}C(p,\pi^+)^{13}C$ leading to the ground and first excited states in ^{13}C for incident proton energies of 159 and 200 MeV.[36,39,40] In these calculations the ground state of ^{13}C is taken to be a single particle $1p_{1/2}$ orbital while the first excited state is described by a $2s_{1/2}$ orbital. The bound state wave functions are generated from potentials with the same radial and diffuseness parameters as for oxygen, namely 1.0 and 0.4 fm, respectively. The optical model parameters used to generate the proton distorted wave are taken from a (class *B*) fit to the $^{12}C(p,p)^{12}C$ data at 150 and 200 MeV.[34,41] In all the calculations presented below the PV form of the vertex has been used.

In Fig. 7 we show the comparison between our results and the observed cross sections. It is evident that the level of agreement with the data is not the same as for the calcium and oxygen cases discussed above. Specifically, the theoretical curves for the ground state transition are well below the data in the forward direction but are a little closer at backward angles. For the first excited state the calculations reproduce the correct shape of the observed cross sections but are almost an order of magnitude below the data, even taking the spectroscopic factor to be unity as we do. We note that this excited state has the same quantum numbers ($2s_{1/2}$) as the 0.87

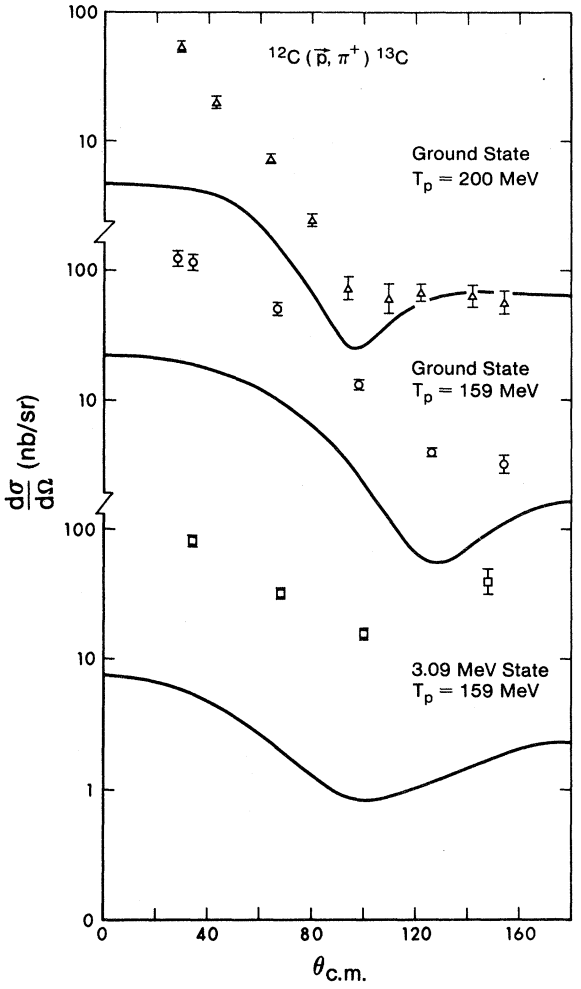

FIG. 7. Cross sections for the reaction $^{12}C(\vec{p},\pi^+)^{13}C$ leading to the ground state in ^{13}C for incident proton energies of 200 and 159 MeV, and leading to the first excited (at 3.09 MeV) state in ^{13}C at $T_p = 159$ MeV. The solid curves are calculated using the PV coupling. The data are from Refs. 36, 39, and 40.

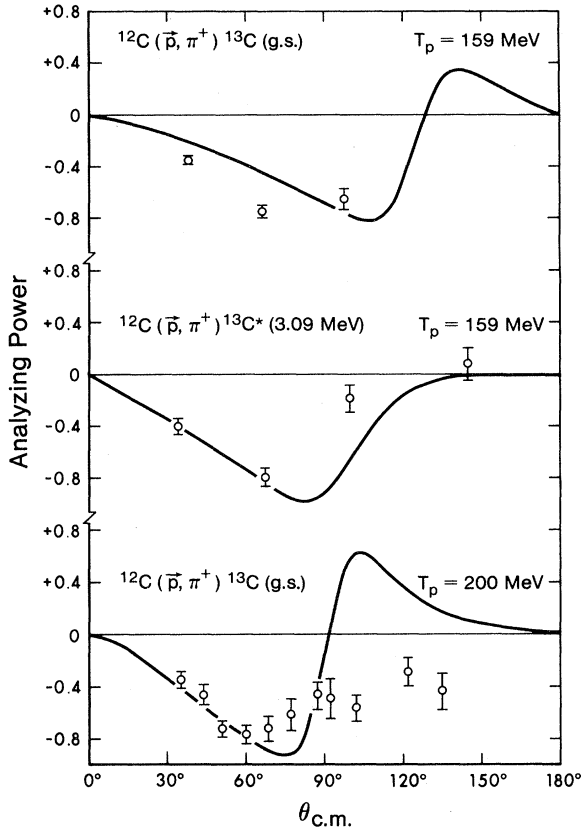

FIG. 8. The analyzing powers for the reaction $^{12}C(\vec{p},\pi^+)^{13}C$ at $T_p = 159$ MeV (for the ground and first excited states in ^{13}C) and at $T_p = 200$ MeV (ground state only). The solid curves are the results of the present calculations using PV coupling. The 200 MeV data are from Ref. 39 and those for 159 MeV are from Ref. 36.

MeV state in ^{17}O where, as mentioned above, the shape of the angular distribution was predicted correctly but the magnitude was down by a factor of 10. Attempts to improve these results by variations in the bound state geometry or through the use of different proton optical potentials have been unsuccessful. It seems more likely that these discrepancies are caused by configuration mixing in the residual nuclear states which renders our extreme single particle description inadequate. Such a possibility is suggested by the work of Miller[42] who has shown that configuration mixing effects in the states of ^{13}C are important in nonrelativistic DWBA calculations.

In Fig. 8 we show the analyzing power predictions and data[36,39] for the above cases. The data are generally negative at forward angles, both for the ground and first excited states. At 159 MeV the curves reproduce this negative trend rather well. At 200 MeV the calculated analyzing power is in good agreement with the data at angles forward of 90°. The curve shows a positive bump at back angles which is not present in the data and which persists even if one uses different bound state geometries or different proton distorting potentials (of course, within the constraint of fitting the relevant proton elastic data). It is interesting to note, however, that a positive bump has been observed in the new TRIUMF data taken at 225 MeV.[43]

Finally, we remark that the analyzing powers for the ground and excited states show some similarity[39] which is indeed borne out by our calculations. This is encouraging to some extent and in effect

strengthens our view that configuration mixing may be responsible for the lack of agreement for the cross sections.

IV. CONCLUSION

In this paper we have introduced an extension of the one nucleon model for (p,π^+) reactions in which both relativistic and distortion effects are taken into account. This has been accomplished, within the DWBA framework, by using Dirac spinors to describe both continuum and bound nucleon states. We find that distortion effects are extremely important. Both proton and pion distortions have significant effects on the calculated cross sections. For the analyzing power it appears that proton distortion plays the more dominant role. Pseudovector and pseudoscalar forms of the $NN\pi$ coupling vertex have been used and we find that the former is invariably in better accord with the data. This is interesting in view of the fact that the pseudovector coupling is the one that satisfies the requirements of PCAC (Miller and Weber[16] have already pointed out that one should adopt the pseudovector coupling). The lack of equivalence between the two types of vertex is understood in terms of the strong nuclear interactions,[23,24] as is shown in Eq. (6). We should note here, however, a new and interesting development by Banerjee and Walker.[45] These authors suggest that, in a fully microscopic approach to pion production and absorption reactions, one should use the pseudoscalar form of the vertex function.

The degree to which our present calculations, with pseudovector coupling, succeed in describing the experimental situation can be summarized as follows:

(i) For reactions on ^{40}Ca and ^{16}O leading to the ground state of the final nucleus, both the shape and magnitude of the angular distributions in the forward hemisphere are reproduced fairly well.

(ii) Two dominant features of the analyzing power data for proton energies below 200 MeV, namely the large negative nature at forward angles and the near similarity of analyzing powers for different final states in ^{13}C, are both reproduced by our calculations.

Our model, however, does not succeed in reproducing the magnitude of the cross sections for reactions leading to the first excited state in ^{17}O and the ground and first excited states in ^{13}C. Configuration mixing may be responsible for part of this discrepancy, particularly for the latter case since we get reasonable results for the analyzing power.

The lack of agreement at large angles, on the other hand, is more likely an indication that some mechanism, other than the ONM, is contributing to the reaction. A likely candidate is the target emission contribution.[6,44]

We, therefore, conclude that for situations where the resulting nuclear state is simple, the ONM is capable of interpreting the data in the forward hemisphere, provided that relativistic effects are properly accounted for. We should, however, point out that more information about relativistic descriptions of nucleon motion in nuclei is required, particularly for excited states and for targets that are not good closed shells. In the course of the present calculations, we have restricted ourselves to one particular pion-nucleus optical potential (the Stricker, McManus, and Carr[18] potential). The extent to which this is justified has not been fully explored. Investigation of other types of potentials should be carried out and we plan to do this in the near future.

ACKNOWLEDGMENTS

The authors wish to thank R. D. Bent for making some of the data used in the present work available to them prior to publication. We are grateful to Jim Easton for many helpful discussions concerning the computational aspects of this work. This work was supported in part by the Natural Sciences and Engineering Research Council of Canada.

---

*Present address: Indiana University Cyclotron Facility, Milo B. Sampson Lane, Bloomington, Indiana 47405.

[1]H. W. Fearing, in *Progress in Particle and Nuclear Physics,* edited by D. Wilkinson (Pergamon, New York, 1981), Vol. 7, p. 113.

[2]D. F. Measday and G. A. Miller, Annu. Rev. Nucl. Part. Sci. 29, 121 (1979).

[3]M. Dillig and M. C. Huber, Phys. Lett. 69B, 429 (1977).

[4]A. M. Green and E. Maqueda, Nucl. Phys. A316, 215 (1979).

[5]Z. Grossman, F. Lenz, and M. P. Locher, Ann. Phys. (N.Y.) 84, 348 (1974).

[6]B. D. Keister and L. S. Kisslinger, contributed paper to the Ninth International Conference on High Energy Physics and Nuclear Structure, Versailles, France, 1981 (unpublished).
[7]M. Ruderman, Phys. Rev. 87, 383 (1952).
[8]H. W. Fearing, Phys. Rev. C 11, 1210 (1975).
[9]M. Tsangarides, Ph. D. thesis, Indiana University, 1979 (unpublished).
[10]M. Tsangarides, J. G. Wills, and R. D. Bent, in *Meson-Nuclear Physics—1979 (Houston),* Proceedings of the 2nd International Topical Conference on Meson-Nuclear Physics, edited by E. V. Hungerford III (AIP, New York, 1979), p. 192.
[11]M. V. Barnhill III, Nucl. Phys. A131, 106 (1969).
[12]J. L. Friar, Phys. Rev. C 10, 955 (1974).
[13]T.-S.H. Lee and S. Pittel, Nucl. Phys. A256, 509 (1976).
[14]L. D. Miller and H. J. Weber, Phys. Lett. 64B, 279 (1976).
[15]R. Brockmann and M. Dillig, Phys. Rev. C 15, 361 (1977).
[16]L. D. Miller and H. J. Weber, Phys. Rev. C 17, 219 (1978).
[17]E. D. Cooper and H. S. Sherif, Phys. Rev. Lett. 47, 818 (1981).
[18]K. Stricker, H. McManus, and J. A. Carr, Phys. Rev. C 19, 929 (1979).
[19]L. D. Miller and A. E. S. Green, Phys. Rev. C 5, 241 (1972).
[20]L. D. Miller, Ann. Phys. (N.Y.) 91, 40 (1975).
[21]R. Brockmann, Phys. Rev. C 18, 1510 (1978).
[22]M. Jaminon, C. Mahaux, and P. Rochus, Phys. Rev. C 22, 2027 (1980).
[23]J. L. Friar, Phys. Rev. C 15, 1783 (1977).
[24]J. V. Noble, Phys. Rev. Lett. 43, 100 (1979).
[25]J. D. Walecka, Ann. Phys. (N.Y.) 83, 491 (1974).
[26]L. G. Arnold, B. C. Clark, and R. L. Mercer, Phys. Rev. C 19, 917 (1979).
[27]L. G. Arnold, B. C. Clark, R. L. Mercer, and P. Schwandt, Phys. Rev. C 23, 1949 (1981).
[28]L. G. Arnold, B. C. Clark, E. D. Cooper, H. S. Sherif, D. A. Hutcheon, P. Kitching, J. M. Cameron, R. P. Liljestrand, R. N. MacDonald, W. J. McDonald, C. A. Miller, G. C. Neilson, W. C. Olsen, D. M. Sheppard, G. M. Stinson, D. K. McDaniels, J. R. Tinsley, R. L. Mercer, L. W. Swenson, P. Schwandt, and C. E. Stronach, Phys. Rev. C 25, 936 (1982).
[29]E. D. Cooper and H. S. Sherif (unpublished).
[30]D. Halderson, R. J. Philpott, J. A. Carr, and F. Petrovich, Phys. Rev. C 24, 1095 (1981).
[31]G. W. Reynaud and F. Tabakin, Phys. Rev. C 23, 2652 (1981).
[32]S. Dahlgren, P. Grafström, B. Höistad, and A. Asberg, Nucl. Phys. A227, 245 (1974).
[33]P. H. Pile, R. D. Bent, R. E. Pollock, P. T. Debevec, R. E. Marrs, M. C. Green, T. P. Sjoreen, and F. Soga, Phys. Rev. Lett. 42, 1461 (1979).
[34]P. G. Roos and N. S. Wall, Phys. Rev. 140, B1237 (1965); C. Rolland, B. Geoffrion, N. Marty, M. Morlet, B. Tatischeff, and A. Willis, Nucl. Phys. 80, 625 (1966); A. Nadasen, P. Schwandt, P. P. Singh, W. W. Jacobs, A. D. Bacher, P. T. Debeveck, M. D. Kaitchuck, and J. T. Meek, Phys. Rev. C 23, 1023 (1981).
[35]T. P. Sjoreen, P. H. Pile, R. D. Bent, M. C. Green, J. J. Kehayias, R. E. Pollock, F. Soga, M. C. Tsangarides, and J. G. Wills, Phys. Rev. C 24, 2569 (1981).
[36]T. P. Sjoreen, P. H. Pile, R. E. Pollock, W. W. Jacobs, H. O. Meyer, R. D. Bent, M. C. Green, and F. Soga, Phys. Rev. C 24, 1135 (1981).
[37]R. Alphonce, A. Johansson, and G. Tibell, Nucl. Phys. 4, 672 (1957).
[38]D. A. Hutcheon and P. Kitching (private communication).
[39]E. G. Auld, A. Haynes, R. R. Johnson, G. Jones, T. Masterson, E. L. Mathie, D. Ottewell, P. Walden, and B. Tatischeff, Phys. Rev. Lett. 41, 462 (1978).
[40]F. Soga, P. H. Pile, R. D. Bent, M. C. Green, W. W. Jacobs, T. P. Sjoreen, T. E. Ward, and A. G. Drentje, Phys. Rev. C 24, 570 (1981).
[41]H. O. Meyer, P. Schwandt, G. L. Moake, and P. P. Singh, Phys. Rev. C 23, 616 (1981).
[42]G. A. Miller, Nucl. Phys. A224, 269 (1974).
[43]G. J. Lolos, P. L. Walden, E. L. Mathie, G. Jones, E. G. Auld, W. R. Falk, R. B. Taylor, Phys. Rev. C 25, 1086 (1982).
[44]W. R. Gibbs, LASL Report No. LA-8303-C, 1980 (unpublished), p. 233.
[45]M. K. Banerjee and G. E. Walker, contributed paper to the Ninth International Conference on High Energy Physics and Nuclear Structure, Versailles, France, 1981 (unpublished); G. E. Walker, private communication; M. K. Banerjee, in *Pion Production and Absorption in Nuclei,* AIP Conf. Proc. No. 79 , edited by R.D. Bent (AIP, New York, 1982).